Impact of Chorda Tympani Nerve Injury on Cell Survival, Axon Maintenance, and Morphology of the Chorda Tympani Nerve Terminal Field in the Nucleus of the Solitary Tract

Rebecca B. Reddaway,* Andrew W. Davidow, Sarah L. Deal, and David L. Hill*

Department of Psychology, University of Virginia, Charlottesville, Virginia 22904

ABSTRACT

Chorda tympani nerve transection (CTX) has been useful to study the relationship between nerve and taste buds in fungiform papillae. This work demonstrated that the morphological integrity of taste buds depends on their innervation. Considerable research focused on the effects of CTX on peripheral gustatory structures, but much less research has focused on the central effects. Here, we explored how CTX affects ganglion cell survival, maintenance of injured peripheral axons, and the chorda tympani nerve terminal field organization in the nucleus of the solitary tract (NTS). After CTX in adult rats, the chorda tympani nerve was labeled with biotinylated dextran amine at 3, 7, 14, 30, and 60 days post-CTX to allow visualization of the terminal field associated with peripheral processes. There was a significant and persistent reduction of the labeled chorda tympani nerve terminal field volume and density in the NTS following CTX. Compared with controls, the volume of the labeled terminal field was not altered at 3 or 7 days post-CTX; however, it was significantly reduced by 44% and by 63% at 30 and 60 days post-CTX, respectively. Changes in the density of labeled terminal field in the NTS paralleled the terminal field volume results. The dramatic decrease in labeled terminal field size post-CTX cannot be explained by a loss of geniculate ganglion neurons or degeneration of central axons. Instead, the function and/or maintenance of the peripheral axonal process appear to be affected. These new results have implications for long-term functional and behavioral alterations. J. Comp. Neurol. 520:2395–2413, 2012.

INDEXING TERMS: taste; gustatory; anterograde; axotomy; biotinylated dextran amine

The morphological integrity of taste buds depends on their innervation. Removal of neural innervation of taste buds by axotomy results in a dramatic loss of taste buds that is reversed upon reinnervation (Cheal and Oakley, 1977; Fujimoto and Murray, 1970; Guagliardo and Hill, 2007; Guth, 1957). Although the majority of taste buds are restored following regeneration of the nerve, taste bud size and cell number are reduced (Guagliardo and Hill, 2007; Oakley et al., 1993; Shuler et al., 2004). This dynamic, innervation-dependent plasticity of taste bud morphology makes the taste system a valuable model system for studies of neuron–target interactions (Sloan et al., 1983; Zalewski, 1974).

The regenerating taste system also provides an excellent model in which to study the plasticity of neuron–target matching. For example, regenerated chorda tympani fibers have decreased branching in taste buds located in fungiform papillae through 6 months postsectioning compared with taste buds with an intact innervation (Montavon et al., 1996), demonstrating that persistent morphological changes within the taste bud remain after nerve regeneration. Moreover, sectioning the chorda tympani nerve (CTX) produces mismatches in the number of neurons that innervate single taste buds (Shuler et al., 2004). Sectioning the chorda tympani nerve or the glossopharyngeal nerve also results in a reduction in the expression of the neurotrophin brain-derived neurotrophic factor (BDNF)

*Rebecca B. Reddaway's present address: Department of Anatomy and Regenerative Biology, The George Washington University, 2300 I Street, NW, Ross Hall 431, Washington, DC 20037.

Grant sponsor: National Institutes of Health; Grant number: R01DC006938.

*CORRESPONDENCE TO: David L. Hill, Department of Psychology, University of Virginia, P.O. Box 400400, Charlottesville, VA 22904-4400. E-mail: dh2t@virginia.edu

Received July 12, 2011; Revised November 2, 2011; Accepted January 7, 2012

DOI 10.1002/cne.23044

Published online January 11, 2012 in Wiley Online Library (wileyonlinelibrary.com)

in taste buds (Ganchrow et al., 2003; Yee et al., 2005). The loss of neurotrophic support could influence cellular processes, such as axonal arborization, synapse formation, and cell survival as seen in the central nervous system (Carter et al., 1998; Cohen-Cory, 1999; Danzer et al., 2002; Niblock et al., 2000; Streppel et al., 2002) and in the peripheral motor and sensory systems following nerve injury (Altschuler et al., 1999; Eriksson et al., 1994; Weibel et al., 1995; Yan et al., 1992) and during regeneration (Kohmura et al., 1999; Lindsay, 1988; Zhang et al., 2000).

Gustatory neurons that sustain profound structural and functional changes peripherally following nerve section also have a central limb. However, relatively few studies have focused on central changes induced by taste nerve injury at adulthood. Documented changes in the first central gustatory relay, the nucleus of the solitary tract (NTS), following nerve damage include long-term transganglionic degeneration (Barry, 1999; Barry and Frank, 1992; Whitehead et al., 1995), incomplete recovery of acetylcholinesterase staining (Barry and Frank, 1992; Barry et al., 2001), and functional taste alterations (Barry, 1999). Although these are pioneering studies, none has detailed the effects on the chorda tympani nerve terminal field that remained after nerve section or identified the upstream events that might underlie the central effects.

In other systems, plasticity of the injured nerve's terminal field commonly occurs after nerve injury and often includes the degeneration of central axons (i.e., transganglionic degeneration), which is linked to the death of cell soma in the sensory ganglion (Arvidsson and Grant, 1979; Arvidsson and Johansson, 1988; Cameron et al., 1992; Florence et al., 1993; Koerber et al., 1994; McMahon and Kett-White, 1991; Molander et al., 1988; Spoendlin, 1984). The degree of changes to the terminal field varies among sensory systems and has been directly related to successful regeneration of neuronal processes and reestablishment of nerve–target relationships that support ganglion cells (e.g., trophic support; Csillik, 1984, 1987; Csillik et al., 1985; Rich et al., 1987, 1989). The current study tests the hypothesis that sectioning the chorda tympani nerve at adulthood leads to a persistent loss of terminal field in the NTS. Moreover, the current study tests the hypothesis that changes in terminal field morphology can at least partially be accounted for by cell death of chorda tympani cells in the geniculate ganglion. We sectioned the right chorda tympani nerve in adult rats and subsequently labeled the nerve at various periods postsectioning. These findings were then extended by examining the effects of unilateral chorda tympani nerve section on the survival of chorda tympani neurons in the geniculate ganglion and maintenance of their peripheral and central neuronal processes (i.e., axons).

MATERIALS AND METHODS

Animals

Adult Sprague-Dawley rats (45–50 days old) were used to examine the central effects of unilateral chorda tympani nerve section. Rats were purchased from Harlan Laboratories (Indianapolis, IN) and housed with food and water available ad libitum. All animal use was endorsed by the Animal Care and Use Committee at the University of Virginia and followed guidelines set by the National Institutes of Health and the Society for Neurosciences.

Chorda tympani nerve transection

Surgical procedures were performed after rats had been sedated with a 0.32 mg/kg injection of Domitor (medetomidine hydrochloride; Pfizer Animal Health, Exton, PA; I.M.) and anesthetized with 40 mg/kg Ketaset (ketamine hydrochloride; Fort Dodge Animal Health, Fort Dodge, IA; I.M.). A warm-water-circulating pad was used to maintain body temperature during surgery. Rats were positioned in a nontraumatic head holder and placed on their backs, and a ventral-medial incision was made in the neck. The digastric and masseter muscles were bluntly dissected to allow the visualization of the right chorda tympani nerve as it bifurcated from the lingual branch of the trigeminal nerve. The chorda tympani nerve was sectioned using sharp microfine forceps; the proximal and distal stumps of the cut chorda tympani nerve were visualized to verify complete transection (Fig. 1). The lingual branch of the trigeminal nerve remained intact. The surgical site was then sutured and infiltrated with 0.04 ml of 0.25% Bupivacaine. Rats were then injected with 1.6 mg/kg Antisedan (atipamezol hydrochloride; Pfizer Animal Health; I.M.) to reverse anesthesia and were allowed to recover on the warm-water-circulating pad before they were returned to their cages. Sham-operated (control) rats underwent the entire surgical protocol; however, the chorda tympani nerve was not transected.

Chorda tympani nerve label

The volume of the chorda tympani nerve terminal field in the NTS was studied via anterograde transport of 3-kD biotinylated dextran amine (BDA; Invitrogen, Carlsbad, CA). To identify changes to the chorda tympani nerve terminal field following CTX, the injured nerve was labeled at 3 ($n = 5$), 7 ($n = 7$), 14 ($n = 8$), 30 ($n = 4$), or 60 ($n = 6$) days post-CTX. For controls, the chorda tympani nerve was labeled 60 days following sham surgery ($n = 8$). To label the chorda tympani nerve, rats were anesthetized and maintained surgically as described above for the CTX. An incision was made on the ventromedial surface of the neck. The ventral portion of the tympanic bulla was

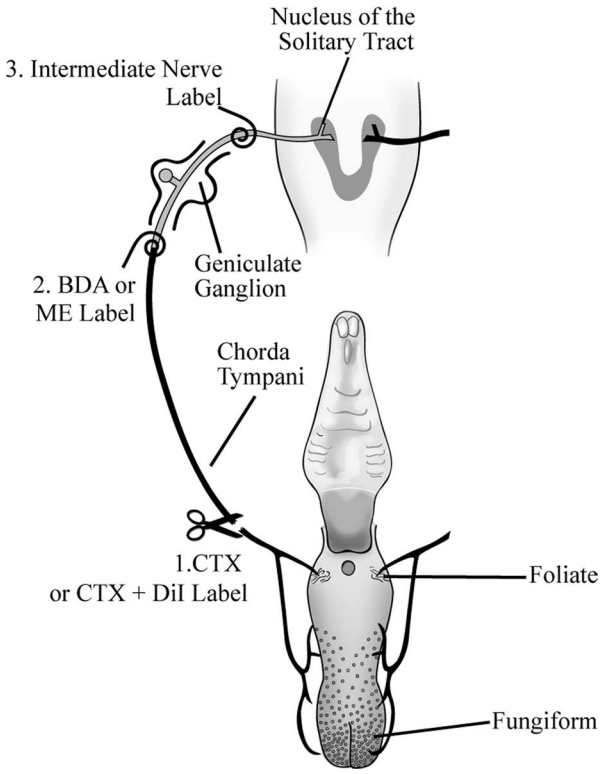

Figure 1. Anatomical organization of the peripheral gustatory system and the first central synaptic relay in the nucleus of the solitary tract (NTS) and the experimental procedures. The chorda tympani nerve innervates taste buds in fungiform and foliate papillae on the anterior tongue and innervates the rostral NTS (shown in horizontal plane). Cell somas of the chorda tympani nerve are located in the geniculate ganglion. 1) The right chorda tympani nerve was sectioned (CTX) in the neck as it bifurcates from the lingual branch of the trigeminal nerve. In some experiments, DiI was applied to the chorda tympani nerve immediately after the CTX. 2) At 3, 7, 14, 30, or 60 days post-CTX, the chorda tympani nerve was labeled with 3-kD biotinylated dextran amine (BDA), which was transported anterogradely to the terminals of the chorda tympani nerve in the NTS. In other experiments, 3-kD micro-emerald (ME) was applied at this site to examine the number of labeled geniculate ganglion cells; BDA was not applied to the nerve in these experiments. 3) The intermediate nerve, which contains the central projection of geniculate ganglion cells, was labeled with BDA to examine the presence of central chorda tympani nerve axons. The palate is shown for reference but is not innervated by the chorda tympani nerve.

exposed, and a hole was made in its surface with a sharp microfine forceps. The chorda tympani nerve was sectioned distal to the geniculate ganglion, and crystals of 3-kD BDA were placed on the proximal stump of the chorda tympani nerve over a 10-minute period (Fig. 1). No attempt was made to deliver the same amount of BDA among rats; rather, the tracer was generously applied to obtain a gelatinous consistency over the entire cut end of the nerve for all animals. This procedure was used in previous studies that yielded terminal field labels in rats of different ages and experimental conditions (Corson and Hill, 2011; Mangold and Hill, 2007; 2008; May and Hill, 2006; Sollars and Hill, 2000; Sollars et al., 2006; Thomas and Hill, 2008). There were no noticeable differences between groups in accessing the chorda tympani nerve or in labeling it with BDA. A piece of parafilm was then placed over the hole made in the ventral portion of the tympanic bulla, and the surgical site was sutured and infiltrated with 0.04 ml of 0.25% Bupivacaine. Rats were then injected with 1.6 mg/kg Antisedan I.M. to reverse anesthesia and were allowed to recover on the warm-water-circulating pad before they were returned to their cages.

Tissue preparation

After a survival period of 24 hours after nerve labeling, rats were deeply anesthetized with 2.4 g/kg urethane (ethyl carbamate; Sigma-Aldrich, St. Louis, MO; I.P.) and transcardially perfused with Krebs-Henseleit buffer (pH 7.3) followed by 8% paraformaldehyde (pH 7.2). Previous work (May and Hill, 2006; Sollars et al., 2006) and pilot experiments showed that this period was optimal for transport of BDA to the NTS. Brains were removed and placed in 8% paraformaldehyde overnight. Brainstems were then blocked and sectioned with a vibratome in the horizontal plane at 50 μm. As in our previous studies of afferent nerve terminal field organization in the NTS, we chose to focus our analyses on horizontal sections of the NTS, because the largest extent of the terminal fields can be visualized in the fewest horizontal planes, in large part because the axons project rostral to caudal and send off terminals medially in approximately the same plane (Corson and Hill, 2011; Lasiter, 1992, 1995; Lasiter and Diaz, 1992; Lasiter and Kachele, 1990; Lasiter et al., 1989; Mangold and Hill, 2007; 2008; May and Hill, 2006; Pittman and Contreras, 2002; Sollars and Hill, 2000; Sollars et al., 2006; Thomas and Hill, 2008). However, analyses of afferent and efferent projections within NTS subdivisions have been made in coronally sectioned tissue (Corson et al., 2011; Whitehead, 1988, 1990, 1993; Whitehead et al., 1993). Therefore, to survey terminal field organization post-CTX with respect to NTS subdivisions, we sectioned an additional two brains in controls and in rats 60 days post-CTX in the coronal plane to examine qualitatively the potential CTX-induced changes within identified subdivisions of the NTS.

Tissue sections were collected in 0.1 M phosphate-buffered saline (PBS; pH 7.2) at room temperature, followed by a 1 hour incubation in PBS containing 0.2% Triton with 1:500 streptavidin Alexa Fluor 488 (Molecular Probes, Eugene, OR) to visualize the BDA-labeled chorda tympani nerve terminal field. Finally, tissue sections were rinsed with PBS and imaged with a confocal laser scanning microscope.

Confocal microscopy and terminal field analyses

Data from fluorescently stained images and analyses of terminal field volumes and densities were similar to data described in detail by Corson and Hill (2011).

Imaging

Briefly, horizontal sections were imaged with an Olympus IX70 microscope fitted with a Fluoview v5.0 laser scanning system (Olympus America, Melville, NY). Optical sections of each 50-μm section containing terminal field were captured sequentially every 3 μm with a ×10 objective (UPlanSApo; NA = 0.40). Image acquisition settings were adjusted so that pixels within the terminal field for each section were just below saturation. Transmitted light images at ×4 (UPlanSApo; NA = 0.13) and at ×10 were captured for each physical section containing the labeled terminal field. This subsequently allowed an accurate registration of similar brainstem sections among animals through the use of common brainstem landmarks (×4) and identification of NTS borders (×10).

For all figure plates, Adobe Illustrator CS5.1 and Photoshop CS5.1 (Adobe Systems, San Jose, CA) were used to compose images from digital files. When appropriate, all optical sections for each physical section were flattened into one plane. Images were enhanced only for contrast and brightness.

Analyses of total terminal field volume

Quantification of terminal field volume and density was achieved through the use of ImageJ software (NIH). Each image stack was initially rotated in ImageJ so that the solitary tract was oriented vertically (Fig. 2). With the corresponding transmitted light image used as a reference, the border of the NTS was outlined for each physical section (shown as black lines in Fig. 2). The image stack was then cropped to include only the NTS (Fig. 2). The maximum entropy thresholder algorithm (Sahoo et al., 1988) was applied to the pixel intensity frequency histogram generated from the entire image stack (i.e., all tiff files of every optical image). This yielded a binary image stack of the pixels above threshold, representing the labeled terminal field. Figure 2 shows the binary image of pixels above threshold in an optical section and represents the data that were analyzed. An analysis was performed to quantify the pixel area above threshold. That is, the number of pixels above threshold for each optical section was summed by ImageJ, converted into area by multiplying the number of pixels by pixel size (1.38 μm × 1.38 μm), and then multiplied by 3 μm (i.e., distance between optical sections) to determine the volume of BDA label (i.e., volume of labeled terminal field) in each physical section.

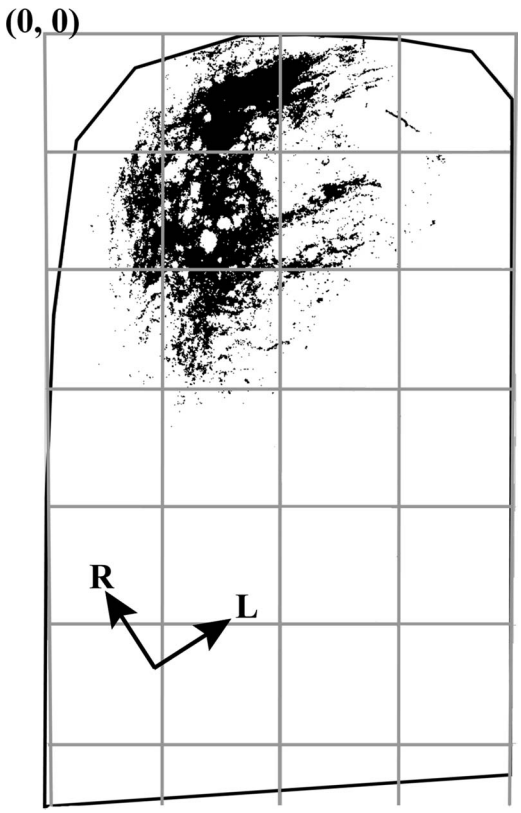

Figure 2. Illustration of density quantification. A binary image of pixels above threshold is shown for an optical section from the physical section shown in Figure 3A. The NTS in the horizontal plane, outlined in black, was subdivided into 200 × 200 pixel uniform grid boxes for density analysis. The columns formed by the grids (see gray boxes) were arranged parallel to the solitary tract (not shown here). The intersection of the leftmost and topmost borders of the NTS in the figure is the 0,0 coordinate. R, rostral; L, lateral. Analyses were done on entire image stacks.

Volumes from each physical section were summed to yield the total terminal field volume for each rat. The resultant volume represents an unbiased-experimenter measure of the amount of label.

Because the diameter of some of the unmyelinated chorda tympani nerve axons may be smaller than the pixel size obtained at ×10 (i.e., <1.38 μm; Whitehead and Frank, 1983), it is possible that we could overestimate the volume of the terminal fields by this method. However, in an earlier report, we found that quantifying the terminal field label in the same region of interest at ×10 and at ×20 (0.69 μm per pixel) yielded volumes within 10% of each other. In fact, the larger volumes were found with the ×20 measurement (Corson and Hill, 2011). We also note that analyses of the label included axons (e.g., the solitary tract) in addition to terminals because of the difficulty of cropping out axons from image stacks.

Geniculate ganglion cell survival and axon maintenance following CTX

Double labeling the chorda tympani nerve

To determine whether there was a progressive loss of geniculate ganglion cells following CTX, we used a double-label fluorescent technique similar to that used to examine dorsal root ganglion cell degeneration in adult rats (Welin et al., 2008). Namely, we used a long-term fluorescent label that was applied to the chorda tympani nerve at the time of CTX. This labeled all of the chorda tympani cells in the geniculate ganglion neurons present at the time of CTX. The chorda tympani nerve was then labeled a second time, but in the tympanic bulla at 14 or 60 days post-CTX with a different fluorescent tracer (Fig. 1). This method allowed us to determine potential changes in the population of geniculate ganglion cells that remained after CTX (i.e., an indication of cell death) and the number of ganglion cells available for labeling at different periods post-CTX (i.e., an indication of regenerated peripheral axons).

We labeled the chorda tympani nerve with 1,1′-dioctadecyl-3,3,3′,3′-tetramethylindocarbocyanine perchlorate (DiI; Invitrogen, Carlsbad, CA) at the time and site of the original CTX. DiI was chosen for the first application because of its persistence in labeled neurons for up to 9 months without an apparent leakage of the tracer into nearby, unlabeled cells and its persistence in the soma of axotomized neurons (Vidal-Sanz et al., 1988). We first placed crystals of DiI on the sectioned nerve in the neck where the chorda tympani nerve normally bifurcates from the lingual branch of the trigeminal nerve (i.e., where the CTX was done for terminal field experiments; Fig. 1). The incision used to gain access to the chorda tympani nerve was sutured as described previously, and the rat recovered from surgery on a heating pad. At 14 ($n = 5$) or 60 ($n = 7$) days post-CTX, the chorda tympani nerve was then exposed in the tympanic bulla and cut, as described previously, and labeled with 3 kD micro-emerald (Invitrogen; Fig. 1). The anesthetic procedure and postsurgical recovery were as described earlier. For control animals, crystals of DiI ($n = 5$) or micro-emerald ($n = 4$) were placed on the sectioned nerve in the neck where the chorda tympani nerve bifurcates from the lingual branch of the trigeminal nerve; no second label was applied. All animals were perfused and fixed 24 hours after final labeling, and the ganglion was removed and postfixed in 8% paraformaldehyde overnight.

The entire ganglion was trimmed from other tissue (e.g., the facial nerve), wet mounted between two coverslips, and imaged as described in the previous section, with the exception that sequential imaging of micro-emerald and DiI was done with a 488-nm blue argon laser and a 543-nm green HE/NE laser, respectively. Optical images were taken every 2 μm. Neurolucida software (version 4.34; MicroBrightField, Colchester, VT) was used to count red (DiI)-, green (micro-emerald)-, or double-labeled cells. All of the cells in each ganglion were examined; therefore, stereological techniques were not used (Shuler et al., 2004).

Double labeling geniculate ganglion cells to examine maintenance of central axons

In contrast to the previous procedure in which the maintenance of peripheral axons post-CTX was assessed, this procedure was designed to examine the number of geniculate ganglion cells of the chorda tympani nerve that sent axons centrally following CTX. As in the previous experiment, we used DiI to label all of the geniculate ganglion cells that were the cell soma of the chorda tympani nerve at the time of the CTX (i.e., the peripheral processes of these cells) and then labeled the intermediate nerve with BDA at 30 days post-CTX (Fig. 1). The intermediate nerve contains the centrally projecting processes of geniculate ganglion soma, which includes soma of the greater superficial petrosal and chorda tympani nerves. Therefore, BDA labeled all of the geniculate ganglion cells that sent a central process through the intermediate nerve. Rats ($n = 3$) were anesthetized again at 30 days post-CTX. The intermediate nerve was exposed in the tympanic bulla by removing a portion of the ventral tympanic bulla, by removing the cochlea, then by removing approximately 2 mm of the petrous portion of the temporal bone. The intermediate nerve was sectioned, and BDA crystals were applied to the distal stump of the cut nerve. After approximately 15 minutes, the area was infiltrated with Kwik-Sil (World Precision Instruments; Sarasota, FL) to maintain contact between the nerve and BDA and to seal fluid from leaking into the site. After a 24-hour survival, rats were perfused, and the geniculate ganglion was extracted and placed in fixative for 2 hours, followed by cryoprotection for 2 hours in 20% sucrose. Cryostat sections (20 μm) of the geniculate ganglion were collected and mounted on slides. Slides were allowed to dry and then placed in 1:500 streptavidin conjugated to Alexa 488 (Invitrogen) in PBS overnight (without Triton).

Long-term labeling of the chorda tympani nerve terminal field

DiI not only has the property of being a long-term retrograde label for cell soma but also labels terminal fields of the chorda tympani nerve in adult rats (Pittman and Contreras, 2002). We labeled the chorda tympani nerve in the neck with DiI (i.e., at the time of CTX; Fig. 1) so that no reaction was needed to visualize and analyze DiI-labeled chorda tympani and then examined the DiI-labeled

terminal fields after 60 days. Thus, our aim was to determine how a terminal field labeled at the time of CTX appeared after 60 days. The surgical and terminal field imaging procedures were as described above, with the exception of terminal fields.

Analyses of terminal field volume and density of label in dorsal-ventral zones

The analysis of terminal field volume and density is the same as detailed by Corson and Hill (2011). Briefly, we identified where the potential reorganization of the chorda tympani nerve terminal field occurred following CTX, and we subdivided the NTS into X, Y, and Z planes. For the medial-lateral and rostral-caudal analyses (X and Y), the NTS in the horizontal plane was subdivided into uniform grid boxes of 200 pixels $\times$ 200 pixels (276 μm $\times$ 276 μm; see gray lines in Fig. 2), with the 0,0 coordinate corresponding to the most rostral and most medial borders of the NTS (Fig. 2). The density of terminal field label was calculated in each grid box for each physical section by dividing the chorda tympani terminal field volume within a grid box by the volume of the portion of the NTS contained within the grid box (i.e., volume of terminal field label/volume of the NTS within the grid box).

We examined the volume of labeled terminal field in five dorsal-ventral zones, each consisting of 100 μm (i.e., two horizontal sections/zone) for terminal field analyses in the dorsal-ventral plane (Z). As noted by us and by others, the orientation of the NTS within the brainstem is such that the caudalmost portion of the NTS is dorsal to the rostralmost portion (see Mangold and Hill, 2007). Therefore, the NTS extends ventrally and rostrally from the dorsalmost extent of the NTS. As a result of this orientation, we chose to combine two 50-μm sections in each zone, thereby permitting analyses of labeled densities among closely aligned regions of interest.

We used the same anatomical criteria to assign each horizontal section to a specific zone as was done for the initial characterization of terminal field densities of the chorda tympani (Corson and Hill, 2011). Zone A is characterized by the sections in which the fourth ventricle occupies the largest medial-lateral extent, in which the solitary tract extends from the rostral pole to the caudal NTS, in which the spinal trigeminal tract extends to near the rostral pole of the NTS, and in which there is a lack of the hypoglossal and facial nuclei. Zone B also has the fourth ventricle extending in the medial-lateral plane, but less so than in zone A; the solitary tract is confined to the caudal portion of the NTS; the NTS extends to near the dorsal cochlear nucleus; and the spinal trigeminal tract extends just rostral to the rostral pole of the NTS. As in zone A, there is no hypoglossal nucleus; however, the dorsalmost extent of the facial nucleus may be present. Zone C is characterized by a significant thinning of the fourth ventricle compared with zones A and B; the solitary tract extends throughout the NTS and is more medially located than in zones A and B; the rostral pole of the NTS extends to the level of dorsal cochlear nucleus; and both the hypoglossal and facial nuclei are evident. The spinal trigeminal tract extends beyond the rostral pole of the NTS in this zone. Zone D is at the level ventral to the fourth ventricle; the NTS has elongated to the midregion of the ventral cochlear nucleus and has narrowed significantly compared with the more dorsal zones. The hypoglossal and facial nuclei are clearly seen in this zone. Finally, in zone E, the borders of the NTS are difficult to distinguish because of the many tracts and neuropil. However, compared with zone D, the NTS extends rostrally to the midrostral-caudal level of the ventral cochlear nucleus. The spinal trigeminal nucleus is less obvious in this zone compared with zone D, and the hypoglossal and facial nuclei are larger and more distinct in this zone compared with the more dorsal zones.

These landmarks were consistent among sham and CTX groups. To check for reliability, a person naïve to the experimental groups assigned sections for each animal into the five zones based on the characterization detailed above, and these were compared with the assignments made by the authors. With minor exceptions, the dorsal-ventral zone assignments among investigators were the same.

Examination of terminal fields in coronal sections

The NTS from two control and two 60 days post-CTX animals were sectioned coronally on a vibratome at 50 μm and imaged as described above with a $\times$10 objective. After terminal fields had been imaged, the tissue was stained for myelin (Schmued and Slikker, 1999) to allow better identification of subdivisions within the NTS. No quantitative measurements were taken.

Statistical analysis

Terminal field volumes

The mean $\pm$ SEM was calculated for the total chorda tympani nerve terminal field volumes for all sections and for terminal field volumes within defined dorsal-ventral zones. Comparisons were made between CTX groups and sham controls using independent-samples *t*-tests. Results with $P < 0.05$ are reported as significant.

Density by dorsal-ventral zones

Density measures for each zone were compared between controls and each CTX group. Each zone was subdivided into a 6 $\times$ 6 (column $\times$ row) grid and analyzed by MANOVA (SPSS; IBM, Somers, NY).

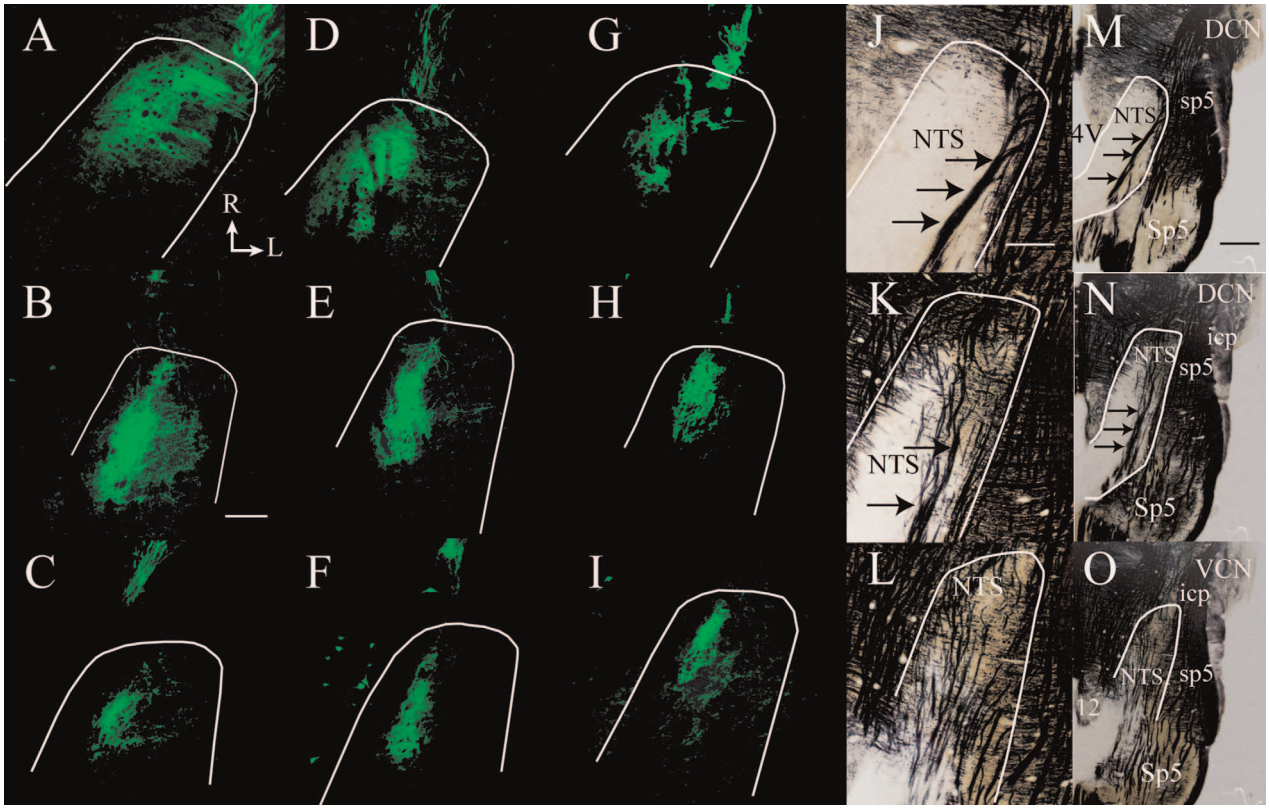

Figure 3. Horizontal sections of labeled CT terminal field (green) from the dorsal through the ventral zones of the rostral NTS. Fluorescent photomicrographs of labeled CT terminal field in a control rat (**A–C**), 7 days post-CTX rat (**D–F**), and 60 days post-CTX rat (**G–I**). The approximate location of NTS is outlined in white. Myelin-stained brainstem sections (Schmued and Slikker, 1999) from a control rat are shown in **J–L** at a similar magnification as shown for A–I and in a lower magnification in **M–O** to illustrate the brainstem landmarks characteristic of dorsal through ventral zones, representing zones B–D, respectively (see text). The location and size of landmarks did not differ qualitatively among groups. Arrows point to the solitary tract in J, K, M, and N. Rostral (R) and lateral (L) are indicated in A. 4V, fourth ventricle; 12, hypoglossal nucleus; DCN, dorsal cochlear nucleus; icp, inferior cerebellar peduncle; NTS, nucleus of the solitary tract; Sp5, spinal trigeminal nucleus; sp5, spinal trigeminal tract; VCN, ventral cochlear nucleus. Scale bars = 200 μm in B (applies to A–I); 200 μm in J (applies to J–L); 1 mm in M (applies to M–O).

RESULTS

Labeling of the chorda tympani nerve in control and CTX animals resulted in strong fluorescent signals in the NTS. The chorda tympani nerve terminal field in control rats appeared qualitatively similar to descriptions from studies that examined chorda tympani nerve terminal fields in adult rats (Fig. 3; Corson and Hill, 2011; Mangold and Hill, 2007, 2008; May and Hill, 2006; Sollars et al., 2006). In all groups, chorda tympani nerve fibers were visible entering the NTS in the rostral pole and terminated in the rostral portion of the NTS (Fig. 3A–I).

Decrease in chorda tympani terminal field volume

CTX in adult rats resulted in a significant and persistent reduction of the labeled chorda tympani nerve terminal field volume in the NTS. To illustrate the reduction of the labeled terminal fields, Figure 3 shows the label in a control rat (Fig. 3A–C) and in a rat with a CTX 7 days (Fig. 3D–F) and 60 days (Fig. 3G–I) prior to terminal field labeling in three dorsal-ventral regions. The landmarks corresponding to these dorsal-ventral planes are shown in myelin-stained tissue (×10, Fig. 3J–L; ×4, Fig. 3M–O). These three regions were subsequently subdivided further into a total of five zones for volume and density analyses (see Materials and Methods). The loss of labeled terminal field volume was not immediate, insofar as the chorda tympani nerve terminal field appeared similar to controls through 7 days post-CTX (Fig. 3A–F). The mean total labeled terminal field volume in rats that survived for 3 and 7 days post-CTX was similar to that of controls, although the mean total labeled terminal field volume in rats 7 days post-CTX was approximately 30% less than that in controls (Fig. 4). By 14 days post-CTX, the total volume of the labeled chorda tympani nerve terminal field was significantly reduced by 44% compared with controls (Fig. 4; $P < 0.05$). Labeled terminal field volume remained

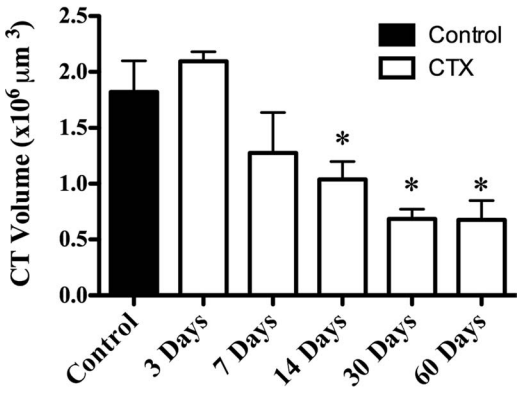

Figure 4. Mean total chorda tympani nerve terminal field volume (±SEM) in control rats (solid bar) and rats 3, 7, 14, 30, and 60 days post-CTX (open bars). Asterisks denote a significant difference ($P < 0.05$) from the control group.

significantly smaller than control at 30 (63% reduction) and 60 (63% reduction) days post-CTX ($P < 0.05$; Fig. 4). Reduction of the volume, although persistent through 60 days (Fig. 3G–I), was not significantly different than that after 14 days ($P > 0.05$; Fig. 4). Therefore, our results indicate a dramatic long-term loss of total labeled chorda tympani nerve terminal field volume following CTX by 14 days post-CTX. This volume reduction did not recover with extended time: we examined the labeled terminal field in rats that survived for as long as 210 days post-CTX and found a small terminal field volume similar to what was seen in the 60 days post-CTX group.

Restriction of terminal field spread throughout the dorsal-ventral axis of NTS

Initially, to examine the distribution of terminal field label, we counted the number of 50 μm horizontal sections that contained terminal field label. The number of sections containing labeled chorda tympani terminal field was reduced in experimental animals by 14 days post-CTX ($P < 0.05$). On average (±SEM), chorda tympani terminal fields were found through 335 (±20) μm of the dorsal-ventral axis at 14 days post-CTX, compared with 418 (±15) μm of the dorsal-ventral axis in controls. The dorsal-ventral spread of terminal fields remained significantly attenuated at 30 days (316 ± 17 μm) and 60 days (341 ± 15 μm) post-CTX ($P < 0.05$), indicating a persistent restriction of labeled terminal field organization throughout the dorsal-ventral extent of the NTS.

Decrease in chorda tympani terminal field volume as it relates to NTS zones: horizontal sections

We originally divided the NTS into five horizontal zones of interest (see Materials and Methods). However, as indicated above, the dorsalmost zone (zone A) contained little terminal field label and was confined to controls and 3 days post-CTX rats. Therefore, for these analyses, we analyzed data from only zones B–E (Fig. 5).

The labeled terminal field in zone B was relatively small, with no differences in mean labeled chorda tympani terminal field volume between any CTX group and controls (Fig. 5A). By contrast, in zone C, the labeled terminal field volumes for 30 and 60 days post-CTX groups decreased by 92% and 82%, respectively, compared with controls (Fig. 5B; $P < 0.01$). Although the magnitude of labeled terminal field change in zone D was not as dramatic as that seen in zone C, the effects were more widespread. In this field, which contains the largest volume of the labeled terminal field, there were significant decreases in labeled terminal field volume compared with controls for all CTX groups, except for the 3-day post-CTX group. Specifically, there was a 52%, 62%, 63%, and a 56% decrease for the 7, 14, 30, and 60 days post-CTX groups, respectively (Fig. 5C; $P < 0.01$). Finally, there were no significant differences between any of the CTX groups and the control group for the most ventral horizontal zone (zone E; Fig. 5D; $P > 0.05$).

Although Figure 3 clearly depicts the decrease in labeled terminal field post-CTX, the information shown in this figure is not directly translatable to the data shown in Figure 5. The terminal field labels shown in Figure 3A–C are from single physical sections contained in zones C–E and are collapsed images of the optical stacks (see Materials and Methods). In contrast, the volumes shown in Figure 5A–D reflect the sum of all labeled pixels within each zone that are composed of multiple optical and physical sections. Therefore, the spread of terminal field label seen in Figure 3A does not necessarily translate into a larger labeled terminal field volume compared with the section shown in Figure 3B because the density of label in Figure 3B is much greater than that in Figure 3A (i.e., more total labeled pixels). As a consequence, the volume of label in zone D (Fig. 5C) for controls is greater than that in zones B and C (Fig. 5A,B).

Alterations in chorda tympani terminal field density as it relates to NTS zones: horizontal sections

Density measurements were made at each of the horizontal zones described above to examine the medial-lateral and rostral-caudal spread of labeled terminal fields (X-Y spread) for each of the groups. We found that there were no differences in labeled terminal field densities between control and the 3 days post-CTX groups. Similarly, there were no differences in labeled terminal field

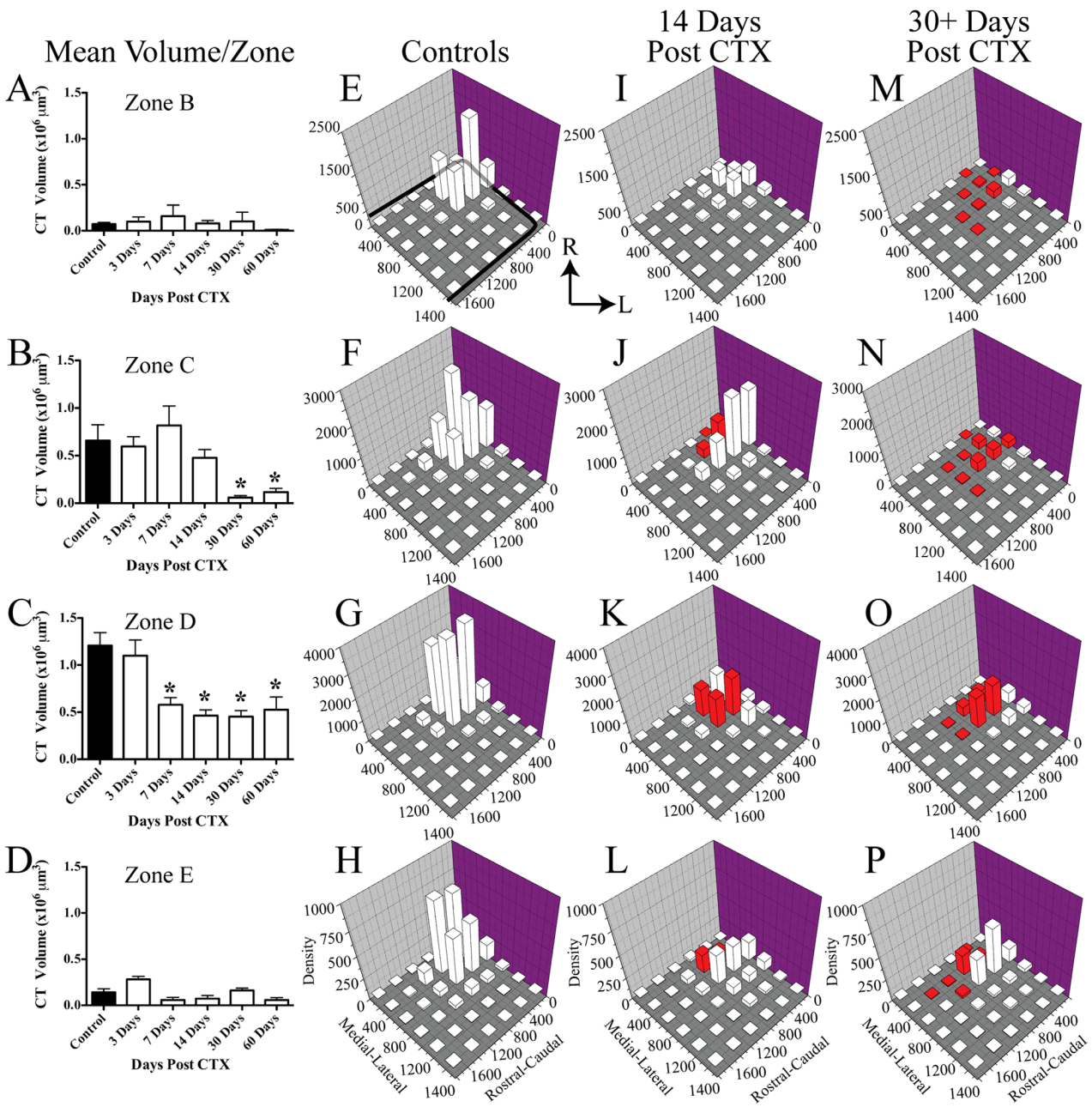

Figure 5. Mean (±SEM) chorda tympani nerve terminal field volumes/zone in control rats (solid bars) and in rats sustaining a CTX at 3, 7, 14, 30 and 60 days (open bars) prior to labeling of the chorda tympani nerve. Data are shown for dorsal to ventral zones B–E (panels **A–D**, respectively). Density of the terminal field label is shown for controls (control and 3 days post-CTX; **E–H**), for 14 days post-CTX rats (**I–L**), and for rats sustaining long-term CTX (30 and 60 days post-CTX; 30+ days post-CTX; **M–P**). Each of the four dorsal-ventral zones is shown by rows, corresponding to the zones shown in A–D. The medial-lateral axis represents distance (micrometers) from the medial border of the NTS, and rostral-caudal axis represents distance (micrometers) from the rostral pole of the NTS (see axis labels in H,L,P). The graphs are oriented along the same axis as the NTS is in the brainstem (see Fig. 3). The solid black line in E represents the outline of the NTS in its greatest extent through the dorsal-ventral axis. Thus, it does not represent the exact width of the NTS for each panel. The z-axis shows the mean density of label and is calculated as the volume of terminal field label/volume of the NTS contained within the respective grid box. See Materials and Methods for further details. Red columns represent $P < 0.05$. R, rostral; L, lateral.

densities between the 30 and 60 days post-CTX groups. Therefore, to present these data more efficiently, we combined the controls and 3 days post-CTX group into the control group (Fig. 5E–H) and the 30 and 60 days post-CTX groups into one long-term CTX group (Fig. 5M–P). All comparisons within a zone were made against the control group (Fig. 5E–H), with significant differences in densities noted as red columns in Figure 5.

As evident from the photomicrographs of the control labeled terminal fields shown in Figure 3A–C, the highest density of label occurred in the rostral-medial portion of the NTS for each zone, with some labeling lateral and caudal to the densest portions of the field (Fig. 5E–H). In zone B (Fig. 5E,I,M), the region of the largest labeled terminal field density in 14 days post-CTX rats and in long-term post-CTX rats was also in the rostral-medial portion of the NTS; however, there was a progressive decrease in the density of this area and surrounding areas compared with controls. In zone B, only the labeled terminal fields in the long-term post-CTX rats (Fig. 5M) were significantly smaller than in controls (Fig. 5E). The progressive decrease in labeled terminal field densities after CTX was also evident in zone C, D, and E (Fig. 5J,N, K,O, L,P, respectively); however, unlike what was seen in zone B, decreases in labeled terminal field densities occurred 14 days post-CTX rats (Fig. 5J–L).

We also analyzed the labeled terminal field density distribution in 7 days post-CTX rats and found some significant decreases in densities compared with controls. The decreases were in the same positions as noted for the 14 days post-CTX group; however, they were not as extensive as in the post-CTX group (data not shown). For example, there were no significant differences in labeled terminal field densities in zone B for the 7 days post-CTX group compared with controls, although the mean densities for this group were intermediate to the controls and 14 days post-CTX. This was the trend for the 7 days post-CTX group in all zones.

In summary, the density measurements consistently showed a progressive decrease in labeled terminal field densities in the rostral-caudal and medial-lateral planes through 30 days post-CTX, at which time the relatively small amount of label was maintained. Moreover, the decreases in labeled terminal field densities were focused primarily at and nearby the densest chorda tympani projection into the NTS in controls. These data generally reflect the corresponding volume changes in label for each zone (Fig. 5A–D) and the qualitative changes seen in the photomicrographs of the labeled terminal fields (Fig. 3A–I).

Decrease in chorda tympani terminal field volume as it relates to NTS subnuclei: coronal sections

The photomicrographs presented in Figure 6 are from a control (Fig. 6A–C) and an experimental (Fig. 6D–F) animal 60 days post-CTX, taken at 2,000 μm (Fig. 6A,D), 1,700 μm (Fig. 6B,E), and 1,400 μm (Fig. 6C,F) rostral to obex (Corson et al., 2011). Boundaries for the subdivisions of NTS subnuclei in Figure 6 are similar to those reported by others (Corson et al., 2011; Halsell et al., 1996) and have been used to describe changes in terminal field volume previously reported from our laboratory (Mangold and Hill, 2007, 2008). It should be noted, however, that there is considerable ambiguity in defining the ventral and lateral borders of the NTS because of the lack of clearly observable differences in myelin staining. This is consistent with the observations of other investigators (e.g., Corson et al., 2011). Moreover, because only a myelin stain was used on the tissue sections containing chorda tympani nerve terminal field label, we were unable to estimate the location of the medial subdivision in coronal sections. This has been accomplished in the past through Nissl-stained tissue (e.g., Corson et al., 2011). Therefore, we show only the outline of the NTS in Figure 6A–D (the most rostral sections) and do not show the medial subdivision in the other, more caudal sections.

In coronal sections of the NTS, the labeled chorda tympani nerve terminal field in controls was found predominantly in the rostral central subdivision of the NTS, but with some label in the rostral lateral subdivision (Fig. 6). In CTX animals, the labeled chorda tympani terminal field was confined almost entirely to the rostral central subdivision of the NTS and was clearly smaller compared with controls (Fig. 6). The exception to this pattern was a lack of chorda tympani nerve terminal field label in the rostral central subdivision in more caudal sections, as illustrated in Figure 6F. Moreover, the labeled terminal field in controls extended more rostrally and caudally than seen in CTX rats (data not shown). Therefore, CTX resulted in an overall decrease of labeled chorda tympani nerve terminal fields, especially in the subdivision that receives the greatest amount of terminal field in control rats.

Injury-induced cell death

Axotomy of sensory nerves at adulthood often leads to the death of their ganglion cells (Aldskogius and Arvidsson, 1978; Aldskogius et al., 1985; Arvidsson and Grant, 1979; Groves et al., 1997; McKay Hart et al., 2002; Morest et al., 1998; Persson et al., 1991; Spoendlin, 1984; Westrum et al., 1976; Zuniga, 1999). A similar loss of geniculate ganglion cells following CTX may account, in part, for the reduced labeled terminal field volume that we show here. To examine this possibility, we employed a double-fluorescence labeling technique to assess the death of geniculate ganglion cells in response to CTX.

Figure 7A shows a photomicrograph of the geniculate ganglion in a rat in which DiI was applied to the chorda tympani nerve when the nerve was cut in the neck and then labeled central to the CTX but still distal to the ganglion (i.e., in the tympanic bulla) with micro-emerald at 60 days post-CTX. The image is a collapsed view of the entire geniculate ganglion; however, each optical section (2-μm

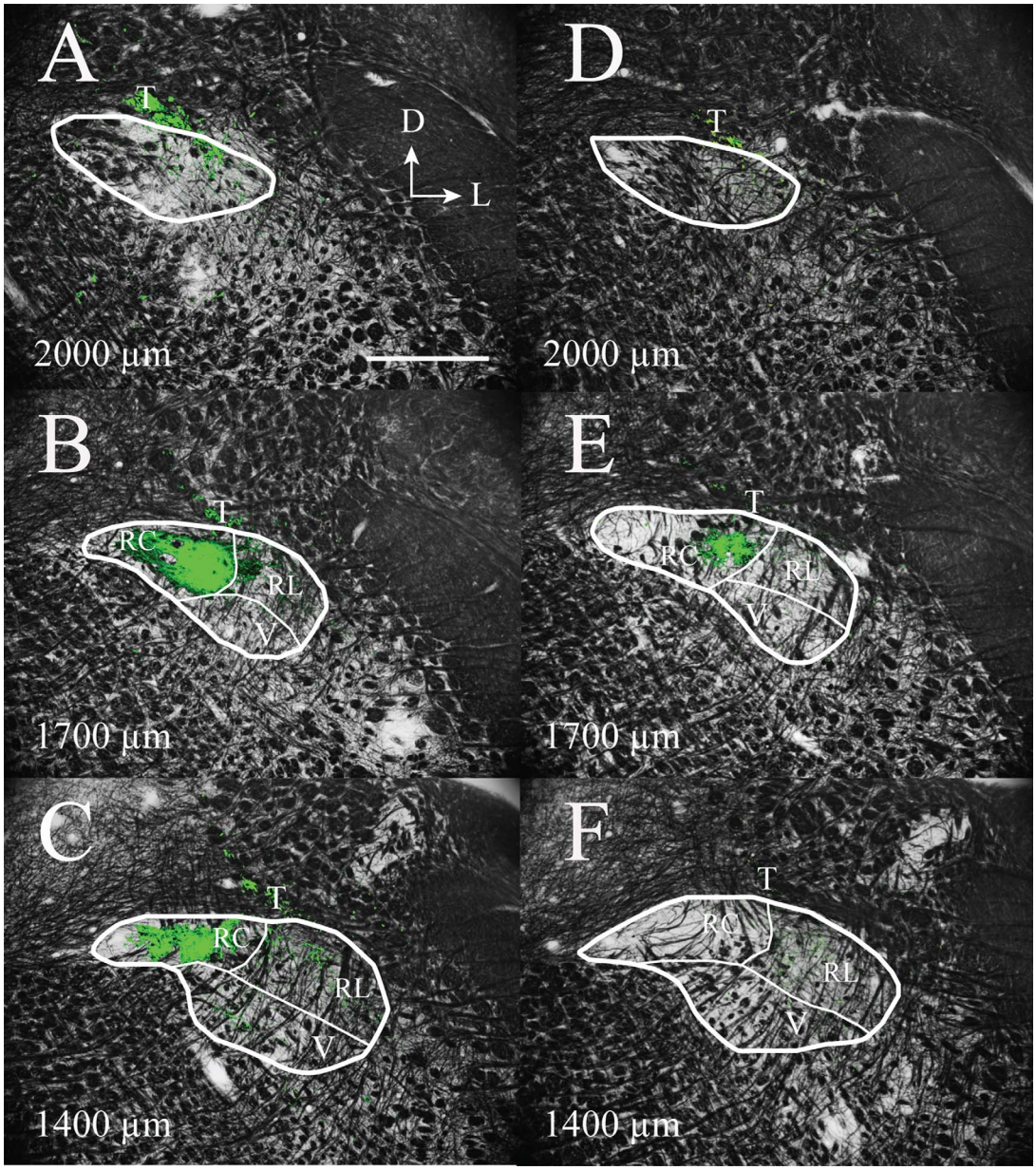

Figure 6. The chorda tympani nerve terminal field within subdivisions of the NTS in coronal sections through adult rat medulla. The labeled chorda tympani nerve terminal field (green) in a control rat (**A–C**) and in a 60 days post-CTX rat (**D–F**) are superimposed on an image of the same section stained for myelin. A and D are from sections 2,000 μm rostral to obex, B and D are from sections 1,700 μm rostral to obex, and C and F are from sections 1,400 μm rostral to obex and are similar to those described by Corson et al. (2011). The myelin-stained sections were used to demarcate the approximate boundaries of subdivisions in the NTS (shown as thin white lines), as described by Halsell et al. (1996), Whitehead (1990), and Corson et al. (2011). The thicker white lines denote the borders of the NTS. The labeled chorda tympani nerve terminal field in the rat 60 days post-CTX (D–F) appears qualitatively reduced compared with adult control rat (A–C). The label was restricted primarily to the RC subdivision of the NTS for the section 1,700 μm rostral to obex (B,E). However, the label found primarily in the RC subdivision in controls was absent in the rat 60 days post-CTX (C,F). D, dorsal; L, lateral; T, solitary tract; RC, rostral central subdivision of the NTS; RL, rostral lateral subdivision of the NTS; V, ventral subdivision of the NTS. Scale bar = 500 μm.

sections through approximately 120 μm) was analyzed for the presence of single DiI (0 days post-CTX; magenta) or micro-emerald (60 days post-CTX; green) label or both (white). In control animals, in which only DiI or micro-emerald was applied 24 hours before collection of the geniculate ganglion for analysis, the number of labeled chorda tympani cells did not differ (Fig. 7B; $P > 0.10$), indicating no difference in the effectiveness of the two tracers to label ganglion cells. In all CTX animals, every micro-emerald labeled cell was also labeled with DiI (see

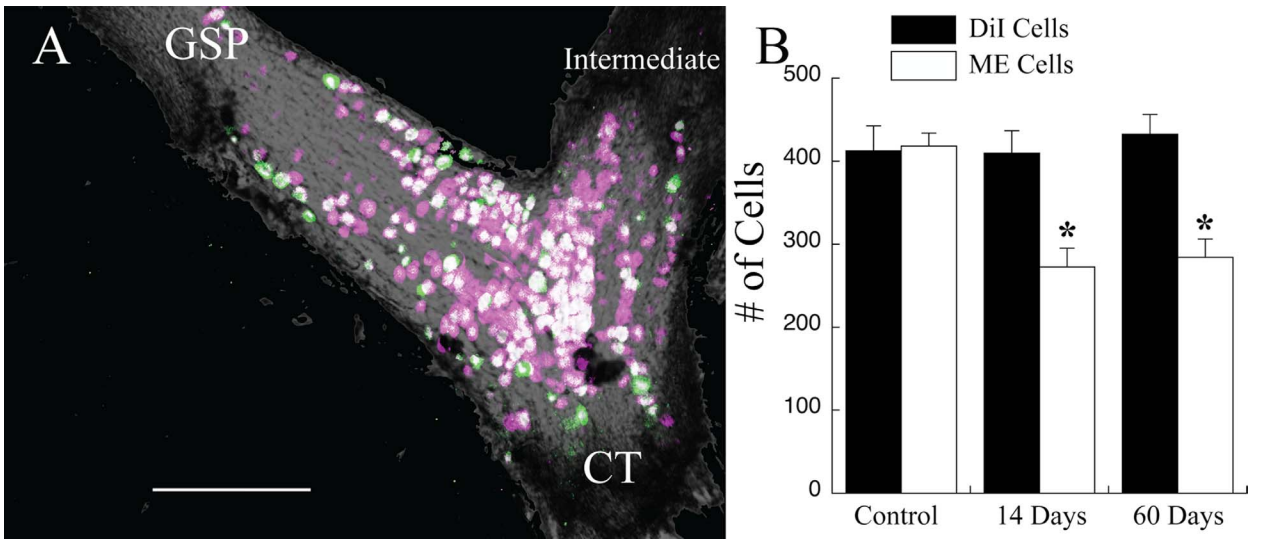

Figure 7. **A:** Photomicrograph of an image stack showing geniculate ganglion cells that were labeled with DiI at the time of the CTX (magenta cells) and those that were labeled with micro-emerald when the nerve was labeled 60 days later (green cells). Magenta-only cells are cells in which peripheral axons were not labeled following the CTX. Double-labeled cells (white cells) are neurons that had peripheral axons at both nerve labeling times. There were no green-only labeled cells. This is a collapsed image; therefore, some cells may obscure the visualization of others. Data were collected from single optical sections. GSP, greater superficial petrosal nerve; CT, chorda tympani nerve; intermediate, intermediate nerve. **B:** Mean (±SEM) number of cells labeled with DiI (solid bars) and with micro-emerald (open bars) in control rats or in rats with a CTX 14 or 60 days before labeling of the chorda tympani nerve with micro-emerald. There was no change in the number of DiI-labeled geniculate ganglion cells post-CTX; however, the number of micro-emerald cells significantly decreased by 14 days post-CTX. *$P < 0.05$ compared with the control group. Scale bar = 200 μm.

Fig. 7A). Moreover, there was no change in the number of DiI labeled cells at 14 or at 60 days post-CTX compared with controls, indicating a resistance to injury-induced cell death (Fig. 7B; $P < 0.05$). In contrast, significant numbers of surviving DiI-labeled cells were not labeled with micro-emerald (Fig. 7B). At 14 days post-CTX, the number of double-labeled cells had significantly decreased by 35% (Fig. 7B; $P < 0.05$) relative to control. There was no further decrease in the proportion of double-labeled cells between 14 days and 60 days post-CTX (Fig. 7B; $P > 0.10$). Taken together, our results indicate that the geniculate ganglion cells of the chorda tympani nerve are resistant to cell death, as evidenced by similar mean numbers of DiI-labeled cells among groups after CTX. The lack of cell death occurs despite the limited availability and/or capability of peripheral chorda tympani axons to transport label by 14 days post-CTX, as evidenced by the reduction in micro-emerald mean cell counts.

We pursued this finding further to see whether chorda tympani ganglion cells in CTX rats sent the peripheral axon into the greater superficial petrosal nerve. This nerve also has its cells in the geniculate ganglion and enters in a location different from that of the chorda tympani nerve. Our methods were the same as described for the cell death experiment, with the exception that micro-emerald was applied to the greater superficial petrosal nerve at 60 days post-CTX instead of to the injured chorda tympani nerve in two rats. In both experiments, none of the geniculate ganglion cells was labeled with both DiI and micro-emerald (data not shown), demonstrating that chorda tympani neurons did not send regenerated peripheral axons into the incorrect nerve.

Apparent lack of injury-induced degeneration of the chorda tympani nerve terminal field

Because found no change in the number of DiI-labeled geniculate ganglion cells after CTX, we sought to determine whether the terminal field labeled with DiI changed post-CTX. We found that there was no significant change in the volume of chorda tympani nerve terminal field when the nerve was labeled with DiI at the time of injury and imaged 60 days later (n = 7; Fig. 8). The mean total terminal field volume of terminal field in the CTX rats was 126% of the control.

Geniculate ganglion cells of the chorda tympani nerve retain centrally projecting axons

The persistence in DiI terminal field volume suggests that the central axons of the transected chorda tympani

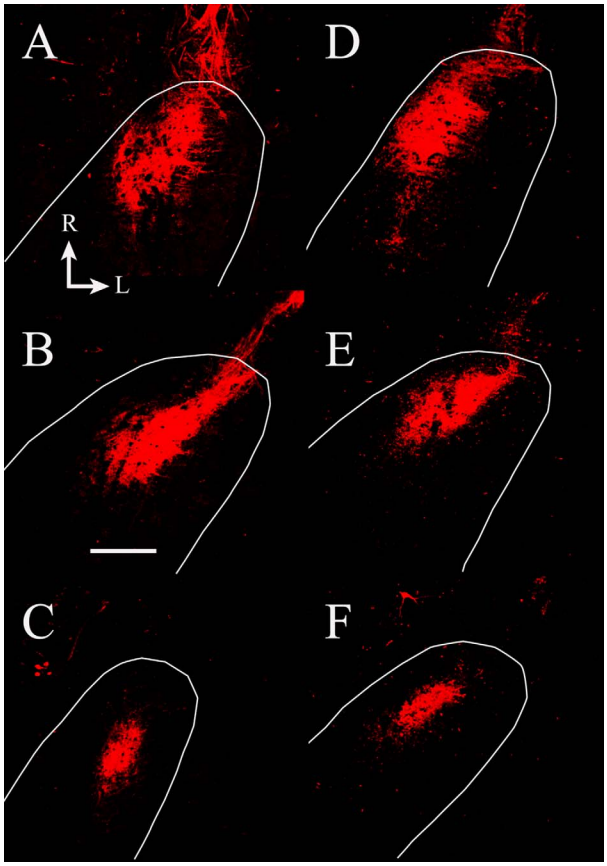

Figure 8. Fluorescent photomicrographs of horizontal sections through the rostral NTS containing DiI-labeled chorda tympani terminal fields in a control rat (**A–C**) and in a 90 days post-CTX rat (**D–F**). The dorsal-ventral levels are the same as shown in Figure 3; A,D represent zone C in Figure 5; B,E represent zone D in Figure 5; C,F represent zone E in Figure 5. The approximate location of NTS is outlined in white. The size and shape of the label are similar between groups. Rostral (R) and lateral (L) are indicated in A. Scale bar = 200 μm.

nerve do not degenerate. To test this hypothesis further, we labeled the chorda tympani nerve with DiI at the time of CTX and then labeled the intermediate nerve (i.e., the central axonal process) with BDA at 30 days post-CTX (Fig. 9). We found that approximately 95% of the DiI-labeled ganglion cells (i.e., chorda tympani cells labeled at the time of CTX) were also labeled with BDA, indicating that nearly all of the cells retained their central axons (Fig. 9).

DISCUSSION

The current study shows that the amount of chorda tympani terminal field in the rat NTS following sectioning of the chorda tympani nerve (CTX), as revealed by labeling the nerve distal to the geniculate ganglion, decreased dramatically with time postsectioning. Decreases in the volume of labeled terminal field do not occur immediately; the changes were not apparent until 14 days post-CTX. The decrease continued so that approximately 60% of the original label volume was lost by 30 days post-CTX. Although there were decreases in labeled terminal field volumes throughout the dorsal to ventral extent of the rostral NTS, the greatest absolute amount of loss in terminal field label occurred in the region that contained the highest density of the terminal field in controls. This region was in the sections at about the middorsal-ventral level of the labeled terminal field. Thus, even though the labeled chorda tympani nerve terminal field volume decreased throughout the NTS, the greatest effect was in the region occupied by the greatest density of terminations in controls. The underlying mechanisms of this loss were likely a cascade of injury-induced processes. We show here, however, that much of the terminal field label following CTX can be attributed to functional and/or morphological changes in the peripheral neuronal process of the chorda tympani nerve (i.e., axon) following CTX and not to a reorganization of the terminal field. Specifically, the geniculate ganglion cells did not die following nerve injury; central processes of the cut nerve appeared to be maintained (i.e., they did not regenerate); and the volume of labeled chorda tympani nerve terminal field present at the time of the CTX was maintained for 60+ days post-CTX.

Several candidate processes might account for the decrease in labeled terminal field volume post-CTX. One is that the injured peripheral process of the chorda

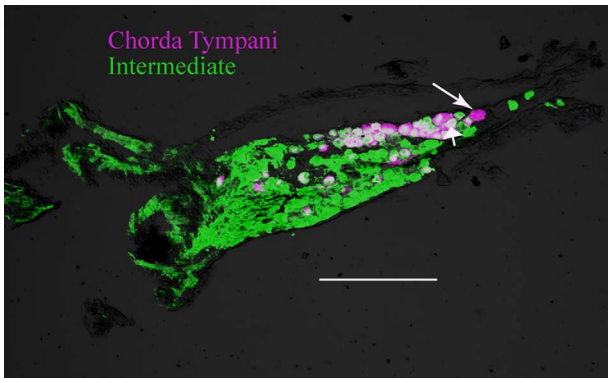

Figure 9. Photomicrograph of a 20-μm section through a geniculate ganglion showing the cells that were labeled at the time of the CTX (DiI-labeled, magenta cells) and all geniculate ganglion cells that send a process centrally through the intermediate nerve (BDA reacted with streptavidin 488, green cells) at 30 days post-CTX. Most (~95%) DiI-labeled cells were also labeled with BDA (double labeled, white), indicating that the chorda tympani neurons that had a peripheral axon at the time of CTX maintained their central process. The long arrow points to a magenta-only cell, and the short arrow points to a double-labeled cell (white cell). Scale bar = 200 μm.

tympani may lose the ability to transport the anterograde tracer with time. Thus, a functional attenuation in the mechanism responsible for transport of BDA may occur after 7 days post-CTX, thereby leading to a lack of tracer in geniculate ganglion cells and in the terminal field. Another is that the decrease in labeled terminal field reflects the progression of injury-induced degeneration of the chorda tympani nerve from the site of the CTX. That is, there may be progressively fewer fibers to label with time as the nerve degenerates, contributing to the decrease in labeled terminal field. Finally, CTX may lead to a failure of the chorda tympani nerve to establish a regenerated axon peripheral to the ganglion. Specifically, ganglion cells would not be lost from injury-induced death, but their ability to maintain a peripheral axon would be lost with time post-CTX. This scenario would result in a reduction of axons peripheral to the ganglion available for labeling by 14 days post-CTX. These hypotheses are not mutually exclusive, and the results may be accounted for by all three processes (and more). We favor the latter two mechanisms to explain the decrease in labeled terminal field volume because of the following observations.

The primary mode of axonal transport of 3-kD dextrans is through fast diffusion (2 mm/hour) along a concentration gradient (Fritzsch, 1993). Pretreatments with colchicine and nocodazole, which depolymerize microtubules, do not impair the ability of dextran tracers to fill neuronal profiles or the speed of this (Fritzsch, 1993). Additionally, dextrans have been successfully used in other systems to examine the success of regeneration over varying periods postnerve cut (Fritzsch and Sonntag, 1991). Most directly related to the current study is recent work in which the chorda tympani nerve terminal field was identified immunohistochemically, showing a reduced terminal field in the mouse NTS following CTX similar to that seen here (Bartel and Finger, 2009). The significance of this is that the nerve was not labeled through nerve sectioning, so no transport of the tracer was involved. Moreover, the results from studies that examined the effects of CTX on taste bud maintenance are consistent with the loss of peripheral axons. Namely, there is a long-term reduction in the number of taste bud cells and taste bud size following CTX in rats (Cain et al., 1996; Cheal and Oakley, 1977; Farbman, 1969; Guagliardo and Hill, 2007; Oakley et al., 1993; Whitehead et al., 1987). Moreover, there is a decrease in numbers of geniculate ganglion cells that innervate single taste buds in CTX rats, as revealed by labeling single fungiform papilla with dextran tracers (Shuler et al., 2004). Therefore, the decrease in size of the peripheral targets of the chorda tympani nerve (i.e., taste buds) is similar to the decrease in volume of the terminal field in CTX rats. Finally, the number of myelinated chorda tympani nerve fibers, as identified through electron microscopy, is less in hamsters sustaining a crush to the nerve compared with controls (Cain et al., 1996), demonstrating that there is an observable loss of axons following nerve injury. In summary, we cannot fully rule out alterations in the effectiveness of the neuronal tracer in CTX rats, but the evidence strongly indicates otherwise.

We also cannot rule out the possibility that the decrease in labeled terminal field after 7 days post-CTX reflects the progressive degeneration of the cut nerve, which was distal to the site of the nerve label (Fig. 1). That is, there may be progressively fewer fibers to label with time as the nerve degenerates. These events may occur for the first 2 weeks; however, most of the degeneration should be completed by this time. By 60 days post-CTX, when the labeled chorda tympani nerve terminal field is the smallest, the nerve will have regenerated, will have innervated taste buds, and functionally will carry taste-elicited signals as seen in multiple species (Cain et al., 1996; Cheal et al., 1977; Cheal and Oakley, 1977; Guagliardo and Hill, 2007). This all occurs in rats before 45 days post-CTX (Hill and Phillips, 1994). Therefore, the reduced labeled chorda tympani field at 60 days post-CTX occurs after functional regeneration of the nerve is established.

Lack of injury-induced cell death and terminal field label

Injury-induced terminal field changes in primary sensory nuclei are also associated with the death of injured sensory neurons in their ganglia (Aldskogius and Arvidsson, 1978; Aldskogius et al., 1985; Arvidsson and Grant, 1979; Groves et al., 1997; McKay Hart et al., 2002; Morest et al., 1998; Persson et al., 1991; Risling et al., 1983; Spoendlin, 1984; Zuniga, 1999). It appears, however, that cell death is not a factor in terminal field changes here. We show that the number of chorda tympani nerve cells in the geniculate ganglion labeled at the time of the CTX does not change over time. A similar conclusion was reported for the adult hamster sustaining CTX (Whitehead et al., 1995). By contrast, labeling the chorda tympani nerve a second time, at least 14 days post-CTX, yields a significantly diminished number of labeled ganglion cells. This result is consistent with our earlier finding that there are approximately 20% fewer geniculate ganglion cells labeled with a neural tracer placed on the chorda tympani nerve distal to the ganglion at 50 days post-CTX (Shuler et al., 2004) and is consistent with the report that there is a significant loss of myelinated fibers in hamsters sustaining a crush to the chorda tympani nerve, even to 16 weeks post-CTX (Cain et al., 1996).

The magnitude of labeled terminal field volume decrease in CTX rats (~60%) compared with controls is much greater than would be predicted by the decrease in number of ganglion cells labeled through the chorda tympani nerve (~20%). This may result from a decrease in the arborization of central axons labeled by way of the chorda tympani nerve. Although this cannot be assessed through the experiments described here and would entail labeling individual chorda tympani neurons, it is clear that the arborization of peripheral axons in taste buds in CTX rats is drastically reduced through 6 months postnerve section (Montavon et al., 1996). Thus, an effect similar to that found in the periphery may be present on the central process of the same nerve.

Comparisons with previous studies on the central consequences of CTX

Previous studies examined the effects of CTX sustained at adulthood on the anatomical properties of the NTS. Studies in adult hamster show that injury to the chorda tympani nerve leads to degeneration within the area of NTS where the nerve forms its terminal field (Barry, 1999; Barry and Frank, 1992; Whitehead et al., 1995), loss of acetylcholinesterase staining (Barry et al., 2001), and a reduction in functional responses to taste stimuli in the NTS at 8 weeks post-CTX (Barry, 1999). Barry (1999) also reported a significant decrease in hamster chorda tympani nerve terminal field density and in terminal field area; however, the region of interest was limited to a 30 μm × 30 μm square in the densest portion of the coronally sectioned terminal field and did not include the entire terminal field. Our results add to these findings by detailing the nature and extent of volume and density changes throughout the entire labeled chorda tympani nerve terminal field following CTX, the time course of labeled terminal field volume and density loss, and the potential underlying mechanisms resident to the geniculate ganglion neurons and to their peripheral and central axons.

The temporal progression of changes in labeled chorda tympani nerve terminal field organization in the adult rat are consistent with the temporal progression of transganglionic degeneration in primary sensory nuclei of other sensory systems (Aldskogius and Arvidsson, 1978; Aldskogius et al., 1985; Arvidsson and Grant, 1979; Morest et al., 1998; Persson et al., 1991; Spoendlin, 1984; Westrum et al., 1976; Zuniga, 1999) as well as that found in the caudal NTS of adult cats (Majumdar et al., 1983). Injury-induced degeneration in primary sensory nuclei in mature animals begins at approximately 3–7 days and is most significant at about 14 days following nerve injury (Aldskogius et al., 1985; Arvidsson and Grant, 1979; Arvidsson et al., 1986; Whitehead et al., 1995).

Consistently with the observations from other systems, we show here that there is a reduction of the labeled chorda tympani nerve terminal field volume at 7 days post-CTX, which is significantly lower than controls by 14 days post-CTX. However, in our case, degeneration does not account for the large loss in terminal field volume. Our data from DiI-labeled rats sustaining CTX indicate that degeneration of chorda tympani cells is not responsible for the extensive loss of labeled terminal field volume, because the DiI-labeled terminal field in rats 60 days post-CTX is similar in volume and topography to controls.

There have been reports, however, that degenerative profiles in the NTS are seen after CTX in hamster (Barry, 1999; Whitehead et al., 1995). We failed to see degenerating profiles in rat (unpublished observations). The apparent difference of our study from others may be due to a variety of factors, including a difference in magnitude of degeneration and species-related differences. It is likely, however, that CTX impacts the cellular environment of the terminal field. A recent report shows that CTX in adult mice triggers in an injury-activated microglial response within the normal zone of the terminal field (Bartel and Finger, 2009), and the time course of the activation is largely similar to the time course of labeled terminal field changes shown here. This may impact degeneration of the terminal field in the mouse NTS. The functional significance of this finding is not known, but such an injury-induced immune response in the central gustatory system may "protect" normal taste function (and perhaps structure) as seen in the periphery (Hill and Phillips, 1994; McCluskey, 2004; Phillips and Hill, 1996).

Physiological and behavioral consequences of the loss in chorda tympani nerve terminal field

The demonstration that there is a long-term decrease in the labeled terminal field volume and density following CTX may have behavioral as well as functional implications. However, it is important to acknowledge that such associations should be interpreted in a restricted manner, because our results are limited to a relatively large-scale morphological reorganization of chorda tympani nerve inputs and do not necessarily include evidence for changes in functional connectivity (i.e., functional synapse number, density, and distribution). More specifically, the decrease in taste-evoked activity in hamster NTS neurons following crush and subsequent regeneration of the hamster chorda tympani nerve (Barry, 1999) may be attributed to an overall loss of afferent input, as suggested by our results, but this does not necessarily mean a proportional loss of functional synapses or a loss of

synapses related to a specific taste modality (e.g., "sour" or "acid").

Correlations between changes in the morphology of chorda tympani nerve terminal field organization and behavior in injured animals are less obvious than correlations between morphology and physiology, but they do provide insights into the plasticity of the injured taste system. In adult animals, unilateral chorda tympani nerve transection produces no changes in behavior (St. John et al., 1995). Bilateral chorda tympani transection is necessary and sufficient to produce significant short-term changes in behavioral taste tests (Spector, 2003; Spector and Grill, 1992; Spector et al., 1990; Spector and Travers, 2005; St. John et al., 1995). However, behavioral alterations in bilaterally transected animals disappear following regeneration of the injured chorda tympani nerves (Kopka et al., 2000; Kopka and Spector, 2001; Spector and Travers, 2005; St. John et al., 1995). This recovery of normal taste-related behaviors indicates that the central taste system is capable of compensating for structural and functional alterations, even though the apparent functional chorda tympani nerve terminal field volume and organization are substantially altered following CTX and the response of postsynaptic targets is attenuated.

By comparison, similar types of overall conclusions can be made with data from rats in which the glossopharyngeal nerve has been transected. Such a transection changes quinine-induced Fos patterns in the NTS and gaping behaviors, which are restored upon nerve regeneration (King et al., 1999, 2000). Thus, if there were decreases in the functional terminal field volume of the glossopharyngeal nerve as seen here for the chorda tympani nerve, recovery of function might also occur as a result of compensatory reactions upon peripheral nerve regeneration.

Plasticity of central taste fields in the NTS

Previous studies that examined the topography and volume of terminal fields of nerves carrying gustatory information following early developmental manipulations found alterations throughout the dorsal-ventral axis of the NTS. The dorsal zone of the NTS is the zone in which the terminal fields of the chorda tympani, greater superficial petrosal, and glossopharyngeal nerves overlap (Mangold and Hill, 2007, 2008; May and Hill, 2006) and is the zone that is most susceptible to many experimental manipulations (Mangold and Hill, 2007, 2008; May and Hill, 2006; Sollars et al., 2006). Because the terminal fields of all three nerves overlap in the rostral NTS, the apparent loss of the functional chorda tympani nerve terminal field in the adult rat following CTX, as was done here, could impact the overall organization of the composite terminal fields. As a result of a reduced functional chorda tympani terminal field, a significant area of synaptic space may allow for the expansion of the intact, fully functional ipsilateral GSP and IX nerve terminal fields. Expansion of neighboring terminal fields following injury in mature animals occurs in gustatory (Corson and Hill, 2011) and nongustatory brainstem regions, including the cuneate nucleus (Jain et al., 2000; Sengelaub et al., 1997), cochlear nucleus (Bilak et al., 1997), and the dorsal horn of the spinal cord (Doubell et al., 1997; LaMotte et al., 1989; Liu and Chambers, 1958; Shehab et al., 2008). Therefore, it is possible that injury-induced plasticity of nerve terminal fields is complex, involving multiple gustatory nerve terminal fields. Such changes may underlie the apparent compensation needed to protect normal taste-elicited behaviors following nerve damage and may be induced in humans through taste nerve damage sustained as a result of disease (Arnold, 1974; Bull, 1965; May and Schlaepfer, 1975), middle ear surgery (Saito et al., 2000, 2001a,b, 2002), or oral surgery (Gent et al., 2003; Schendel and Epker, 1980).

ACKNOWLEDGMENT

We thank Dr. Alev Erisir for assisting us in drawing borders of the NTS in coronal sections.

LITERATURE CITED

Aldskogius H, Arvidsson J. 1978. Nerve cell degeneration and death in the trigeminal ganglion of the adult rat following peripheral nerve transection. J Neurocytol 7:229–250.

Aldskogius H, Arvidsson J, Grant G. 1985. The reaction of primary sensory neurons to peripheral nerve injury with particular emphasis on transganglionic changes. Brain Res 357:27–46.

Altschuler RA, Cho Y, Ylikoski J, Pirvola U, Magal E, Miller JM. 1999. Rescue and regrowth of sensory nerves following deafferentation by neurotrophic factors. Ann N Y Acad Sci 884:305–311.

Arnold SM. 1974. The vulnerability of the chorda tympani nerve to middle ear disease. J Laryngol Otol 88:457–466.

Arvidsson J, Grant G. 1979. Further observations on transganglionic degeneration in trigeminal primary sensory neurons. Brain Res 162:1–12.

Arvidsson J, Johansson K. 1988. Changes in the central projection pattern of vibrissae innervating primary sensory neurons after peripheral nerve injury in the rat. Neurosci Lett 84:120–124.

Arvidsson J, Ygge J, Grant G. 1986. Cell loss in lumbar dorsal root ganglia and transganglionic degeneration after sciatic nerve resection in the rat. Brain Res 373:15–21.

Barry MA. 1999. Recovery of functional response in the nucleus of the solitary tract after peripheral gustatory nerve crush and regeneration. J Neurophysiol 82:237–247.

Barry MA, Frank ME. 1992. Response of the gustatory system to peripheral nerve injury. Exp Neurol 115:60–64.

Barry MA, Haglund S, Savoy LD. 2001. Association of extracellular acetylcholinesterase with gustatory nerve terminal fibers in the nucleus of the solitary tract. Brain Res 921: 12–20.

Bartel DL, Finger TE. 2009. Microglial response in the nucleus of the solitary tract after chorda tympani nerve injury [abstract]. Chem Senses 34:A31.

Bilak M, Kim J, Potashner SJ, Bohne BA, Morest DK. 1997. New growth of axons in the cochlear nucleus of adult chinchillas after acoustic trauma. Exp Neurol 147:256–268.

Bull TR. 1965. Taste and the chorda typani. J Laryngol Otol 79:479–493.

Cain P, Frank ME, Barry MA. 1996. Recovery of chorda tympani nerve function following injury. Exp Neurol 141: 337–346.

Cameron AA, Pover CM, Willis WD, Coggeshall RE. 1992. Evidence that fine primary afferent axons innervate a wider territory in the superficial dorsal horn following peripheral axotomy. Brain Res 575:151–154.

Carter DA, Bray GM, Aguayo AJ. 1998. Regenerated retinal ganglion cell axons form normal numbers of boutons but fail to expand their arbors in the superior colliculus. J Neurocytol 27:187–196.

Cheal M, Oakley B. 1977. Regeneration of fungiform taste buds: temporal and spatial characteristics. J Comp Neurol 172:609–626.

Cheal M, Dickey WP, Jones LB, Oakley B. 1977. Taste fiber responses during reinnervation of fungiform papillae. J Comp Neurol 172:627–646.

Cohen-Cory S. 1999. BDNF modulates, but does not mediate, activity-dependent branching and remodeling of optic axon arbors in vivo. J Neurosci 19:9996–10003.

Corson SL, Hill DL. 2011. Chorda tympani nerve terminal field maturation and maintenance is severely altered following changes to gustatory nerve input to the nucleus of the solitary tract. J Neurosci 31:7591–7603.

Corson J, Aldridge A, Wilmoth K, Erisir A. 2011. A survey of oral cavity afferents to the rat nucleus tractus solitarii. J Comp Neurol (in press).

Csillik B. 1984. Nerve growth factor regulates central terminals of primary sensory neurons. Z Mikrosk Anat Forsch 98:11–16.

Csillik B. 1987. Transganglionic regulation of the primary sensory neuron. Acta Physiol Hung 69:355–361.

Csillik B, Schwab ME, Thoenen H. 1985. Transganglionic regulation of central terminals of dorsal root ganglion cells by nerve growth factor (NGF). Brain Res 331:11–15.

Danzer SC, Crooks KR, Lo DC, McNamara JO. 2002. Increased expression of brain-derived neurotrophic factor induces formation of basal dendrites and axonal branching in dentate granule cells in hippocampal explant cultures. J Neurosci 22:9754–9763.

Doubell TP, Mannion RJ, Woolf CJ. 1997. Intact sciatic myelinated primary afferent terminals collaterally sprout in the adult rat dorsal horn following section of a neighbouring peripheral nerve. J Comp Neurol 380:95–104.

Eriksson NP, Lindsay RM, Aldskogius H. 1994. BDNF and NT-3 rescue sensory but not motoneurones following axotomy in the neonate [see comments]. Neuroreport 5: 1445–1448.

Farbman AI. 1969. Fine structure of degenerating tast buds after denervation. J Embryol Exp Morphol 22:55–68.

Florence SL, Garraghty PE, Carlson M, Kaas JH. 1993. Sprouting of peripheral nerve axons in the spinal cord of monkeys. Brain Res 601:343–348.

Fritzsch B. 1993. Fast axonal diffusion of 3000 molecular weight dextran amines. J Neurosci Methods 50:95–103.

Fritzsch B, Sonntag R. 1991. Sequential double labelling with different fluorescent dyes coupled to dextran amines as a tool to estimate the accuracy of tracer application and of regeneration. J Neurosci Methods 39:9–17.

Fujimoto S, Murray RG. 1970. Fine structure of degeneration and regeneration in denervated rabbit vallate taste buds. Anat Rec 168:383–413.

Ganchrow D, Ganchrow JR, Verdin-Alcazar M, Whitehead MC. 2003. Brain-derived neurotrophic factor-, neurotrophin-3-, and tyrosine kinase receptor-like immunoreactivity in lingual taste bud fields of mature hamster after sensory denervation. J Comp Neurol 455:25–39.

Gent JF, Shafer DM, Frank ME. 2003. The effect of orthognathic surgery on taste function on the palate and tongue. J Oral Maxillofac Surg 61:766–773.

Groves MJ, Christopherson T, Giometto B, Scaravilli F. 1997. Axotomy-induced apoptosis in adult rat primary sensory neurons. J Neurocytol 26:615–624.

Guagliardo NA, Hill DL. 2007. Fungiform taste bud degeneration in C57BL/6J mice following chorda-lingual nerve transection. J Comp Neurol 504:206–216.

Guth L. 1957. The effects of glossopharyngeal nerve transection on the circumvallate papilla of the rat. Anat Rec 128: 715–730.

Halsell CB, Travers SP, Travers JB. 1996. Ascending and descending projections from the rostral nucleus of the solitary tract originate from separate neuronal populations. Neuroscience 72:185–197.

Hill DL, Phillips LM. 1994. Functional plasticity of regenerated and intact taste receptors in adult rats unmasked by dietary sodium restriction. J Neurosci 14:2904–2910.

Jain N, Florence SL, Qi HX, Kaas JH. 2000. Growth of new brainstem connections in adult monkeys with massive sensory loss. Proc Natl Acad Sci U S A 97:5546–5550.

King CT, Travers SP, Rowland NE, Garcea M, Spector AC. 1999. Glossopharyngeal nerve transection eliminates quinine-stimulated fos-like immunoreactivity in the nucleus of the solitary tract: implications for a functional topography of gustatory nerve input in rats. J Neurosci 19:3107–3121.

King CT, Garcea M, Spector AC. 2000. Glossopharyngeal nerve regeneration is essential for the complete recovery of quinine-stimulated oromotor rejection behaviors and central patterns of neuronal activity in the nucleus of the solitary tract in the rat. J Neurosci 20:8426–8434.

Koerber HR, Mirnics K, Brown PB, Mendell LM. 1994. Central sprouting and functional plasticity of regenerated primary afferents. J Neurosci 14:3655–3671.

Kohmura E, Yuguchi T, Yoshimine T, Fujinaka T, Koseki N, Sano A, Kishino A, Nakayama C, Sakaki T, Nonaka M, Takemoto O, Hayakawa T. 1999. BDNF atelocollagen minipellet accelerates facial nerve regeneration. Brain Res 849:235–238.

Kopka SL, Spector AC. 2001. Functional recovery of taste sensitivity to sodium chloride depends on regeneration of the chorda tympani nerve after transection in the rat. Behav Neurosci 115:1073–1085.

Kopka SL, Geran LC, Spector AC. 2000. Functional status of the regenerated chorda tympani nerve as assessed in a salt taste discrimination task. Am J Physiol Regul Integr Comp Physiol 278:R720–R731.

LaMotte CC, Kapadia SE, Kocol CM. 1989. Deafferentation-induced expansion of saphenous terminal field labelling in the adult rat dorsal horn following pronase injection of the sciatic nerve. J Comp Neurol 288:311–325.

Lasiter PS. 1992. Postnatal development of gustatory recipient zones within the nucleus of the solitary tract. Brain Res Bull 28:667–677.

Lasiter PS. 1995. Effects of orochemical stimulation on postnatal development of gustatory recipient zones within the nucleus of the solitary tract. Brain Res Bull 38:1–9.

Lasiter PS, Diaz J. 1992. Artificial rearing alters development of the nucleus of the solitary tract. Brain Res Bull 29: 407–410.

Lasiter PS, Kachele DL. 1990. Effects of early postnatal receptor damage on development of gustatory recipient

zones within the nucleus of the solitary tract. Brain Res Dev Brain Res 55:57–71.

Lasiter PS, Wong DM, Kachele DL. 1989. Postnatal development of the rostral solitary nucleus in rat: dendritic morphology and mitochondrial enzyme activity. Brain Res Bull 22:313–321.

Lindsay RM. 1988. Nerve growth factors (NGF, BDNF) enhance axonal regeneration but are not required for survival of adult sensory neurons. J Neurosci 8:2394–2405.

Liu CN, Chambers WW. 1958. Intraspinal sprouting of dorsal root axons; development of new collaterals and preterminals following partial denervation of the spinal cord in the cat. AMA Arch Neurol Psychiatry 79:46–61.

Majumdar S, Mills E, Smith PG. 1983. Degenerative and regenerative changes in central projections of glossopharyngeal and vagal sensory neurons after peripheral axotomy in cats: a structural basis for central reorganization of arterial chemoreflex pathways. Neuroscience 10: 841–849.

Mangold JE, Hill DL. 2007. Extensive reorganization of primary afferent projections into the gustatory brainstem induced by feeding a sodium-restricted diet during development: less is more. J Neurosci 27:4650–4662.

Mangold JE, Hill DL. 2008. Postnatal reorganization of primary afferent terminal fields in the rat gustatory brainstem is determined by prenatal dietary history. J Comp Neurol 509:594–607.

May M, Schlaepfer WM. 1975. Bell's palsy and the chorda tympani nerve: a clinical and electron microscopic study. Laryngoscope 85:1957–1975.

May OL, Hill DL. 2006. Gustatory terminal field organization and developmental plasticity in the nucleus of the solitary tract revealed through triple-fluorescence labeling. J Comp Neurol 497:658–669.

McCluskey LP. 2004. Up-regulation of activated macrophages in response to degeneration in the taste system: effects of dietary sodium restriction. J Comp Neurol 479:43–55.

McKay Hart A, Brannstrom T, Wiberg M, Terenghi G. 2002. Primary sensory neurons and satellite cells after peripheral axotomy in the adult rat: timecourse of cell death and elimination. Exp Brain Res 142:308–318.

McMahon SB, Kett-White R. 1991. Sprouting of peripherally regenerating primary sensory neurones in the adult central nervous system. J Comp Neurol 304:307–315.

Molander C, Kinnman E, Aldskogius H. 1988. Expansion of spinal cord primary sensory afferent projection following combined sciatic nerve resection and saphenous nerve crush: a horseradish peroxidase study in the adult rat. J Comp Neurol 276:436–441.

Montavon P, Hellekant G, Farbman A. 1996. Immunohistochemical, electrophysiological, and electron microscopical study of rat fungiform taste buds after regeneration of chorda tympani through the non-gustatory lingual nerve. J Comp Neurol 367:491–502.

Morest DK, Kim J, Potashner SJ, Bohne BA. 1998. Long-term degeneration in the cochlear nerve and cochlear nucleus of the adult chinchilla following acoustic overstimulation. Microsc Res Techniq 41:205–216.

Niblock MM, Brunso-Bechtold JK, Riddle DR. 2000. Insulin-like growth factor I stimulates dendritic growth in primary somatosensory cortex. J Neurosci 20:4165–4176.

Oakley B, Lawton A, Riddle DR, Wu LH. 1993. Morphometric and immunocytochemical assessment of fungiform taste buds after interruption of the chorda-lingual nerve. Microsc Res Techniq 26:187–195.

Persson JK, Aldskogius H, Arvidsson J, Holmberg A. 1991. Ultrastructural changes in the gracile nucleus of the rat after sciatic nerve transection. Anat Embryol 184:591–604.

Phillips LM, Hill DL. 1996. Novel regulation of peripheral gustatory function by the immune system. Am J Physiol 271: R857–R862.

Pittman DW, Contreras R. 2002. Dietary NaCl influences the organization of chorda tympani neurons projecting to the nucleus of the solitary tract in rats. Chem Senses 27: 333–341.

Rich KM, Luszczynski JR, Osborne PA, Johnson EM Jr. 1987. Nerve growth factor protects adult sensory neurons from cell death and atrophy caused by nerve injury. J Neurocytol 16:261–268.

Rich KM, Disch SP, Eichler ME. 1989. The influence of regeneration and nerve growth factor on the neuronal cell body reaction to injury. J Neurocytol 18:569–576.

Risling M, Aldskogius H, Hildebrand C, Remahl S. 1983. Effects of sciatic nerve resection on L7 spinal roots and dorsal root ganglia in adult cats. Exp Neurol 82:568–580.

Sahoo PK, Soltani S, Wong KC, Chen YC. 1988. A survey of thresholding techniques. Comput Vis Graphics Image Process. p 233–260.

Saito T, Shibamori Y, Manabe Y, Yamagishi T, Yamamoto T, Ohtsubo T, Saito H. 2000. Morphological and functional study of regenerated chorda tympani nerves in humans. Ann Otol Rhinol Laryngol 109:703–709.

Saito T, Manabe Y, Shibamori Y, Yamagishi T, Igawa H, Tokuriki M, Fukuoka Y, Noda I, Ohtsubo T, Saito H. 2001a. Long-term follow-up results of electrogustometry and subjective taste disorder after middle ear surgery. Laryngoscope 111:2064–2070.

Saito T, Shibamori Y, Manabe Y, Yamagishi T, Igawa H, Yamamoto T, Ohtsubo T, Saito H. 2001b. Intraoperative identification of regenerated chorda tympani nerve and its relationship to recovered taste function. ORL J Otorhinolaryngol Rel Spec 63:359–365.

Saito T, Shibamori Y, Manabe Y, Yamagishi T, Igawa H, Ohtsubo T, Saito H. 2002. Incidence of regeneration of the chorda tympani nerve after middle ear surgery. Ann Otol Rhinol Laryngol 111:357–363.

Schendel SA, Epker BN. 1980. Results after mandibular advancement surgery: an analysis of 87 cases. J Oral Surg 38:265–282.

Schmued L, Slikker W Jr. 1999. Black-gold: a simple, high-resolution histochemical label for normal and pathological myelin in brain tissue sections. Brain Res 837:289–297.

Sengelaub DR, Muja N, Mills AC, Myers WA, Churchill JD, Garraghty PE. 1997. Denervation-induced sprouting of intact peripheral afferents into the cuneate nucleus of adult rats. Brain Res 769:256–262.

Shehab SA, Al-Marashda K, Al-Zahmi A, Abdul-Kareem A, Al-Sultan MA. 2008. Unmyelinated primary afferents from adjacent spinal nerves intermingle in the spinal dorsal horn: a possible mechanism contributing to neuropathic pain. Brain Res 1208:111–119.

Shuler MG, Krimm RF, Hill DL. 2004. Neuron/target plasticity in the peripheral gustatory system. J Comp Neurol 472: 183–192.

Sloan HE, Hughes SE, Oakley B. 1983. Chronic impairment of axonal transport eliminates taste responses and taste buds. J Neurosci 3:117–123.

Sollars SI, Hill DL. 2000. Lack of functional and morphological susceptibility of the greater superficial petrosal nerve to developmental dietary sodium restriction. Chem Senses 25:719–727.

Sollars SI, Walker BR, Thaw AK, Hill DL. 2006. Age-related decrease of the chorda tympani nerve terminal field in the nucleus of the solitary tract is prevented by dietary sodium restriction during development. Neuroscience 137: 1229–1236.

Spector AC. 2003. The functional organization of the peripheral gustatory system: lessons from behavior. In: Fluharty SJ, Grill HJ, editors. Progress in Psychobiology and Physiological Psychology. San Diego: Academic Press. p 101–161.

Spector AC, Grill HJ. 1992. Salt taste discrimination after bilateral section of the chorda tympani or glossopharyngeal nerves. Am J Physiol 263:R169–R176.

Spector AC, Travers SP. 2005. The representation of taste quality in the mammalian nervous system. Behav Cogn Neurosci Rev 4:143–191.

Spector AC, Schwartz GJ, Grill HJ. 1990. Chemospecific deficits in taste detection after selective gustatory deafferentation in rats. Am J Physiol 258:R820–R826.

Spoendlin H. 1984. Factors inducing retrograde degeneration of the cochlear nerve. Ann Otol Rhinol Laryngol Suppl 112: 76–82.

St. John SJ, Markison S, Spector AC. 1995. Salt discriminability is related to number of regenerated taste buds after chorda tympani nerve section in rats. Am J Physiol 269: R141–R153.

Streppel M, Azzolin N, Dohm S, Guntinas-Lichius O, Haas C, Grothe C, Wevers A, Neiss WF, Angelov DN. 2002. Focal application of neutralizing antibodies to soluble neurotrophic factors reduces collateral axonal branching after peripheral nerve lesion. Eur J Neurosci 15:1327–1342.

Thomas JE, Hill DL. 2008. The effects of dietary protein restriction on chorda tympani nerve taste responses and terminal field organization. Neuroscience 157:329–339.

Vidal-Sanz M, Villegas-Perez MP, Bray GM, Aguayo AJ. 1988. Persistent retrograde labeling of adult rat retinal ganglion cells with the carbocyanine dye dil. Exp Neurol 102: 92–101.

Weibel D, Kreutzberg GW, Schwab ME. 1995. Brain-derived neurotrophic factor (BDNF) prevents lesion-induced axonal die-back in young rat optic nerve. Brain Res 679:249–254.

Welin D, Novikova LN, Wiberg M, Kellerth JO, Novikov LN. 2008. Survival and regeneration of cutaneous and muscular afferent neurons after peripheral nerve injury in adult rats. Exp Brain Res 186:315–323.

Westrum LE, Canfield RC, Black RG. 1976. Transganglionic degeneration in the spinal trigeminal nucleus following removal of tooth pulps in adult cats. Brain Res 101: 137–140.

Whitehead MC. 1988. Neuronal architecture of the nucleus of the solitary tract in the hamster. J Comp Neurol 276: 547–572.

Whitehead MC. 1990. Subdivisions and neuron types of the nucleus of the solitary tract that project to the parabrachial nucleus in the hamster. J Comp Neurol 301: 554–574.

Whitehead MC. 1993. Distribution of synapses on identified cell types in a gustatory subdivision of the nucleus of the solitary tract. J Comp Neurol 332:326–340.

Whitehead MC, Frank ME. 1983. Anatomy of the gustatory system in the hamster: central projections of the chorda tympani and the lingual nerve. J Comp Neurol 220: 378–395.

Whitehead MC, Frank ME, Hettinger TP, Hou LT, Nah HD. 1987. Persistence of taste buds in denervated fungiform papillae. Brain Res 405:192–195.

Whitehead MC, McPheeters M, Savoy LD, Frank ME. 1993. Morphological types of neurons located at taste-responsive sites in the solitary nucleus of the hamster. Microsc Res Techniq 26:245–259.

Whitehead MC, McGlathery ST, Manion BG. 1995. Transganglionic degeneration in the gustatory system consequent to chorda tympani damage. Exp Neurol 132:239–250.

Yan Q, Elliott J, Snider WD. 1992. Brain-derived neurotrophic factor rescues spinal motor neurons from axotomy-induced cell death. Nature 360:753–755.

Yee C, Bartel DL, Finger TE. 2005. Effects of glossopharyngeal nerve section on the expression of neurotrophins and their receptors in lingual taste buds of adult mice. J Comp Neurol 490:371–390.

Zalewski AA. 1974. Trophic functions of the neuron. VI. Other trophic systems. Neuronal and tissue specifications involved in taste bud formation. Ann N Y Acad Sci 228: 344–349.

Zhang JY, Luo XG, Xian CJ, Liu ZH, Zhou XF. 2000. Endogenous BDNF is required for myelination and regeneration of injured sciatic nerve in rodents. Eur J Neurosci 12: 4171–4180.

Zuniga JR. 1999. Trigeminal ganglion cell response to mental nerve transection and repair in the rat. J Oral Maxillofac Surg 57:427–437.